WILEY PROTEINS

RESEARCH ARTICLE

Monitoring transient events in infrared spectra using local mode analysis

Matthias Massarczyk[1] | Jürgen Schlitter[1] | Carsten Kötting[1] | Till Rudack[1,2] | Klaus Gerwert[1,2]

[1]Department of Biophysics, Ruhr University Bochum, Bochum, Germany

[2]Chinese Academy of Sciences–Max-Planck Partner Institute for Computational Biology (PICB), Shanghai Institutes for Biological Sciences (SIBS), Shanghai, China

Correspondence
Klaus Gerwert, Department of Biophysics, Ruhr University, Bochum, Germany.
Email: gerwert@bph.rub.de;
and
Till Rudack, Department of Biophysics, Ruhr University, Bochum, Germany.
Email: till.rudack@rub.de

Funding information
Deutsche Forschungsgemeinschaft, Grant/Award Number: 321722360

Abstract

Time-resolved Fourier transformed infrared (FTIR) spectroscopy of chemical reactions is highly sensitive to minimal spatiotemporal changes. Structural features are decoded and represented in a comprehensible manner by combining FTIR spectroscopy with biomolecular simulations. Local mode analysis (LMA) is a tool to connect molecular motion based on a quantum mechanics simulation with infrared (IR) spectral features and vice versa. Here, we present the python-based software tool of LMA and demonstrate the novel feature of LMA to extract transient structural details and identify the related IR spectra at the case example of malonaldehyde (MA). Deuterated MA exists in two almost equally populated tautomeric states separated by a low barrier for proton transfer so IR spectra represent a mixture of both states. By state-dependent LMA, we obtain pure spectra for each tautomeric state occurring within the quantum mechanics trajectory. By time-resolved LMA, we obtain a clear view of the transition between states in the spectrum. Through local mode decomposition and the band-pass filter, marker bands for each state are identified. Thus, LMA is beneficial to analyze the experimental spectra based on a mixture of states by determining the individual contributions to the spectrum and motion of each state.

KEYWORDS

computational chemistry, LMA, malonaldehyde, molecular dynamics simulations, proton transfer, QM, QM/MM, software tool, theoretical IR spectroscopy, time-resolved, vibrational spectroscopy

1 | INTRODUCTION

Structural insights on the sub-Angström level are essential for understanding molecular reaction mechanisms in great detail.[1] Vibrational spectroscopy explores molecular structures with highest spatiotemporal resolution. Smallest changes even in the sub-Ångstrom regime in bond length are revealed by shifts in vibrational frequency.[2] However, the complexity of geometrical changes and the coupling of vibrations prevent the direct determination of the structure from the spectrum. To analyze such small changes unambiguously, a thorough analysis using theoretical approaches is needed. A combination of theoretical quantum mechanics (QM) (or quantum mechanics/molecular mechanics [QM/MM] for larger systems) and experimental approaches in vibrational spectroscopy is well suited to connect atomic structural

properties with spectral features. This combination is well-established and has been demonstrated in many applications.[3–12]

Using time-resolved Fourier transformed infrared (FTIR) difference spectroscopy, it is possible to study the structural transitions and reaction steps in proteins in short time periods. This already enabled a deeper understanding of various reaction mechanisms, such as the light-driven proton pump bacteriorhodopsin[13] or the GTPase mechanism of the Ras protein.[14] To eliminate the irrelevant absorptions, FTIR difference spectroscopy is utilized. As a result, the variable parts caused by protein function are obtained.

Recently, we introduced local mode analysis (LMA).[15] LMA yields the theoretical FTIR spectrum from a single QM or QM/MM trajectory. However, both the contributions of selected atoms to the complete IR spectrum (local mode decomposition [LMD]) and the

contributions of atom motion to a selected spectral band (band-pass filter [BPF]) are identified and represented by LMA.

LMA is now publicly accessible as a python-based software tool, which can be downloaded at https://github.com/MatthiasMa/Local-Mode-Analysis and up-to-date information are available at http://www.bph.rub.de/link_software_en.htm. In this publication, we give an overview of the LMA features including their theoretical background. We provide the required workflow and give details how to access all capabilities of the method. In addition, we introduce state-dependent LMA: During molecular dynamics simulations, different states of the molecule are sampled including conformational changes or even molecular reactions. The different states are identified and differentiated either by structural parameters or by selected features of the spectrum acquired from a time-resolved LMA analysis. As a result, separate IR-spectra of each of the pure states are obtained. We showcase the capabilities of LMA by applying it to the popular model system for studying proton transfer; malonaldehyde (MA) and a deuterated analogue.[16–30]

2 | MATERIALS AND METHODS

Theoretical spectroscopy is based on the electric dipole moment calculated from a pure QM simulation of the QM region from a QM/MM simulations. The simulation generates classical trajectories of all nuclei using energy gradients of the QM region and force-field gradients of the environment. For protons, this approximation does not describe proton transfer kinetics with sufficient accuracy but yields acceptable vibrational spectra as will be shown the following. Dipole moments result from the total density distribution of nuclei and electrons. This impedes spatial localization of molecular movements by assignment to bands in the spectrum, which is necessary to understand the origin of IR spectra.

Here, LMA makes use of a partial charge (PC) model that approximates the total dipole moment $\mathbf{\mu}_{QM}(t)$ from the QM part of the simulation by $\mathbf{m}_{PC}(t)$, which is a sum of atomic moments $\mathbf{s}_k(t)$ calculated at each time step from coordinates $\mathbf{r}_k(t)$ and partial charges $q_k(t)$ as

$$\mathbf{s}_k(t) = q_k(t) \cdot \mathbf{r}_k(t) \tag{1}$$

For all further steps, we refer to the former publication.[15] The model allows the assignment of local motions to the spectrum by LMD and of spectral features to the molecular dynamics by band-pass filtering. The agreement between the IR spectra

$$A_{QM}(\omega) \propto \omega^2 F_\omega [\langle \mathbf{\mu}(0) \cdot \mathbf{\mu}(t) \rangle] \tag{2}$$

derived from $\mathbf{\mu}_{QM}(t)$ and

$$\begin{aligned} A_{PC}(\omega) &\propto \omega^2 F_\omega [\langle \mathbf{m}(0) \cdot \mathbf{m}(t) \rangle] \\ &\propto \omega^2 \mathbf{m}(\omega) \cdot \mathbf{m}^*(\omega) \\ &= \sum_{kl} \underbrace{\omega^2 \mathbf{s}_k(\omega) \cdot \mathbf{s}_l^*(\omega)}_{S_{kl}}. \end{aligned} \tag{3}$$

derived from $\mathbf{m}_{PC}(t)$ is a prerequisite for the decomposition of the spectra. This agreement should always be checked for the system of interest. Note that Equation (2) applies to the complete spectrum including high frequencies because, in the simulation, the nuclei follow classical trajectories with a statistics that obeys the equipartition theorem.[7]

2.1 | Time-dependent LMA

Time-dependent LMA aims at analyzing spectra of systems that undergo transitions. It decomposes the trajectory based on the given number of time windows into subsequent segments of the same length L, which are separately evaluated. Therefore, the distance between segments is homogenous and segments can overlap. The segments have to be long enough to gain a stable IR spectrum and short enough to capture configurational states separated by transition events. Stable IR spectrum means a smooth change between time segments without transition.

2.2 | State-dependent LMA

The state-dependent LMA analyses the trajectory for selected geometric features and decides whether the given feature meets the criteria for the desired state. One defines a function $d(t)$ by

$$d(t) = \begin{cases} 1 & \text{if criterion is met} \\ 0 & \text{else} \end{cases} \tag{4}$$

for selecting state-dependent contributions. It is smoothed by a Gaussian filter to become $\hat{d}(t)$. This smoothed function is applied to $\mathbf{s}_k(t)$ as multiplier to get atomic moments

$$\hat{\mathbf{s}}_k(t) = \hat{d}(t) \cdot \mathbf{s}_k(t) \tag{5}$$

for the selected state. Application of LMA to $\hat{\mathbf{s}}_k(t)$ provides the IR spectrum and the decomposition of the isolated state. Once the IR spectra of different states are obtained, differential IR-spectra can be generated by subtracting the IR spectrum of one state from another one.

2.3 | Simulation setup

The QM simulations were carried out for 3-hydroxy-2-propanal MA and the singular deuterated MA in vacuum. We used TeraChem[31] at the level of camB3LYP (6-31G*) for the simulations. Both simulation systems have no boundaries. To equilibrate the two systems a 5 ps, QM simulation with 0.5 fs step size was performed followed by a QM production run of 100 ps with 0.5 fs step size leading to 200 000 frames that were analyzed by LMA. The simulations were carried out using Langevin dynamics[32] and NpT conditions with 273.15 K and 0.0 bar using thermal coupling to the Langevin thermostat with a collision frequency of 5 ps^{-1}. The point charges, which were used to calculate the atomic moments are Mulliken charges,[33] which are calculated for every step of the simulation.

2.4 | Normal mode analysis

The normal mode spectra were obtained by the QM program suite TeraChem[31] with QM-optimized structures. For both processes, the camB3LYP functional and the 6-31G* basis set were used.

2.5 | Data processing

LMA uses the fast Fourier transformation (FFT) algorithm for FT.[34] In the default mode used in this work, all spectra were calculated using a window function prior to the FT. The time-resolved spectra are composed of 100 5 ps long time segments.

All trajectories were fitted by superimposing the center of mass of all atoms to fit the translation but not the rotation.

All wavenumbers in spectra generated by LMA were scaled by 0.96 to correct the error of the camB3LYP (6-31G*) functional.[35,36]

The Gaussian filter used in the figures had a full width at half maximum of four wavenumbers for LMA and 10 wavenumbers for normal mode analysis (NMA).

2.6 | Used software packages

The LMA python (Python Software Foundation, https://www.python.org/) package makes extensive use of the numpy[37] package for processing. For file input and output, LMA uses mdtraj[38] allowing to use a variety of different trajectory file formats. All plots are created with the Python package matplotlib.[39] The used color palette was optimized by Brewer for color-blind readers with deuteranopia.[40] All structure figures are created using PyMOL.[41]

3 | RESULTS AND DISCUSSION

In the following, we introduce the capabilities and usage of our here developed python-based software tool for LMA. We give a general workflow how to use LMA to connect molecular motion based on a molecular dynamics simulation with IR spectral features and vice versa. Finally, we showcase the benefits of the novel state-dependent and time-resolved LMA features by identifying and separating the time-dependent relationship between spectrum and atomic motion for two distinct proton transfer-dependent states of MA.

3.1 | Capabilities

LMA contains four main modules: LMD, band-pass filter (BPS), time-resolved LMA, and state-dependent LMA. These modules including their key functionalities described in the following are made available in a user-friendly way through a command line based python tool. The key input is a three-dimensional trajectory file, which can be weighted by a one-dimensional time series file. These files are processed within LMA by the autocorrelation function to obtain different types of vibrational spectra depending on the weighting.

3.2 | Local mode decomposition

The local mode decomposition uses an approximation of the total dipole moment from the QM part of the simulation by a sum of atomic dipole moments calculated at each time step from coordinates and partial charges (Equation (3)). This approach allows breaking down IR spectra into individual fractions directly attributable to their local origin. Thus, LMD calculates spectra directly derived from single atom motion (atomic spectra) or from vibrational modes (mode spectra) so

that a direct connection between spectrum and local motion is possible.

Atomic spectra reveal the contribution of each individual atom within the IR spectrum. The interpretation of spectra is usually based on NMA. To make our approach more comparable to NAM, we introduced the mode spectra. When it comes to assigning certain vibrational types within the spectrum, the contributions of atoms are translated into vibrational modes. Each of this vibrational modes has a corresponding bond and one of three possible orthogonal directions. Thus, each bond has one stretching and two bending directions. The bending directions orientate on the neighboring atoms to separate into an out-of-plane and an in-plane direction. This partition enables a generalized translation into the intuitive and common stretching, bending, and torsional vibration modes of molecules as described in detail in our former publication.[15]

To obtain all atomic and mode spectra of the QM region at least the trajectory of coordinates, the time-series of the corresponding partial charges to weight the coordinates and a topology file need to be passed to LMA. A spectrum based on time-independent constant partial charges is obtained by weighting the coordinate trajectory file with the averaged partial charges. A mass weighted mechanical vibrational spectrum where the charge influence is completely removed is obtained if no weighting file is hand over to LMA, which means a weighting of all entries with one. The $A_{QM}(\omega)$ spectrum that is derived from the total wave function dipole moment $\mu_{QM}(t)$ is obtained by passing solely the trajectory of the QM dipole moment of the total QM region as input file to the LMA.

3.3 | Band-pass filter

The BPF goes in the reverse direction as the LMD by deriving molecular motion within the simulation trajectory just for a specific part of the spectrum. BPF provides immediate access to structural information encrypted in the IR spectrum by visualizing the oscillation of molecular structures within a selected spectral band. The BPF uses the atomic coordinates of the simulation trajectory, which are reduced in Fourier space for the desired frequency band followed by Fourier-back-transformation. The BPF is similar to the visualization of normal mode vibrations, but it is derived from the data out of an MD simulation so the resulting trajectory consists of all translations, rotations, and conformational changes in addition to the desired vibrations. Thus, molecular vibrations and their changes are visualized over the course of time in correspondence to chemical reactions or other transition processes occurring as shown in the Supporting Information SM1 [https://youtu.be/ombxxCvtUAw].

To obtain a coordinate trajectory reflecting the atomic oscillations for a selected spectral region, the trajectory of coordinates and a topology file needs to be hand over to LMA as well as the BPS mode needs to be enabled and the spectral region that should be analyzed needs to be specified.

3.4 | Time-resolved LMA

The time-resolved LMA monitors different states of the molecule that are sampled because of conformational changes or reactions like

proton transfer during the simulation and marker bands for these states can be identified. Here, the trajectory is divided into time segments that are continuously evaluated by LMD. From the spectra of the individual time segments, a temporal course of the spectrum is obtained, which makes it possible to investigate molecular events in the spectrum and compare them with the experiment. Time-resolved LMA is beneficial for interpreting different states in experimental FTIR spectra and also enables us to analyze kinetics of reactions.

To obtain a three-dimensional time-resolved IR spectra, the time resolved mode needs to be enabled and the number of time windows must be specified.

3.5 | State-dependent LMA

State-dependent LMA allows extracting one distinct IR spectrum corresponding to each of the different identified states. Individual states are identified and isolated within the trajectory by defining thresholds for specific molecular properties such as geometry. Subsequently, theoretical spectra are calculated from the respective states.

To obtain a pure spectrum of just one distinct state defined by the existence of an individual bond, the switch bond option needs to be enabled. The argument for the switch bond option is the bond number, which is also displayed in the bond.info file that is written out by default for any kind of LMA run containing a topology file.

3.6 | Workflow

The general workflow for employing LMA to connect spectral features with structural motion to identify and to characterize the transient events starts with the validation to use LMA with a certain method for the determination of partial charges for the system of interest. The basic prerequisite for employing LMA is that the calculated total spectrum $A_{PC}(\omega)$ based on the partial charges $\mathbf{m}_{PC}(t)$ agrees with experimental data or if no experimental data are available at least with the calculated spectrum $A_{QM}(\omega)$ based on the total QM dipole moment. The accordance of $A_{PC}(\omega)$ and $A_{QM}(\omega)$ also justifies the spectral decomposition for the used partial charge model for the QM part of the simulation. If these requirements are fulfilled, the spectra can be decomposed into individual atom or mode spectra with LMD or the atomic motions corresponding to specific spectral bands can be extracted by the BPF. To identify different states, the simulation trajectory is first investigated regarding possible different states. Key geometrical changes, for example, the existence of certain bonds, are used to define different states. In the case of proton transfer, the geometrical feature is defined by which atom forms the bond to the proton. Each section of the trajectory is assigned to one of the states by state-dependent LMA and separate spectra for each state are obtained based on the defined geometry feature. Next, marker bands that are only present in one state are identified by comparing the different spectra. These marker bands are assigned to specific vibrational modes through the BPF or LMD. Finally, the shifts of the assigned marker bands within IR spectra can be correlated with the change of the geometrical features over time by time-resolved LMA.

3.7 | Case study: Malonaldehyde

We showcase the capabilities of LMA in the case example of Z-3-hydroxy-prop-2-en-al, usually referred to as MA. MA[17,18,20–30] is a small enol tautomer, which is already well understood and a popular model system. Already 35 years ago, MA was studied with theoretical and experimental IR spectrocopy[19] with a later improved band assignment.[16] Furthermore, it is perfectly suited to demonstrate the benefits of LMA to extract transient structural details as MA exists in two equally populated tautomeric states separated by a low barrier for proton transfer. This low proton transfer barrier allows observing both states within only a few ps QM simulation trajectory. A structural distinguishability of the otherwise degenerated states is achieved by specific isotopic labelling.

3.8 | Validation

First, we compare the calculated total spectrum $A_{PC}(\omega)$ of MA with the experimental IR spectra of gaseous MA.[21] Figure 1 reveals that the calculated spectrum reproduces the experimental one very well, indicating that the derived Mulliken partial charges are sufficient
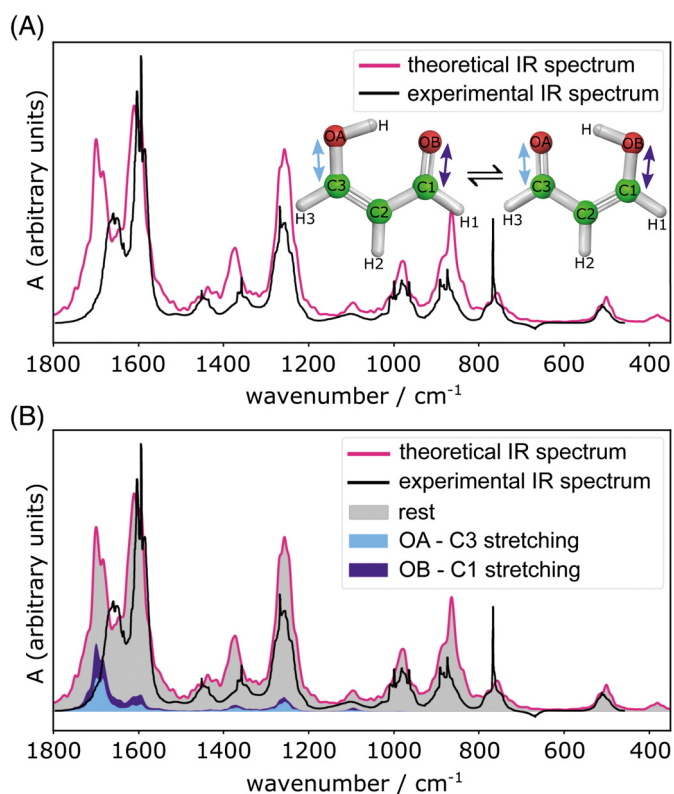

FIGURE 1 IR spectrum of malonaldehyde. A, The theoretical IR spectrum $A_{PC}(\omega)$ (pink) of MA derived by LMA from a 100 ps QM simulation in comparison with the experimental IR spectrum[21] (black) of MA. B, Shown are exemplary vibrational modes obtained by LMD. Like in experiments, frequent proton transfer leads to an equal population of the tautomer with the proton bound to OA and OB, respectively. The shares of the OA—C3 (blue) and the OB—C1 stretching vibrations (purple) on the total spectrum are the same, because both bonds frequently interchange from single bond to double bond [Color figure can be viewed at wileyonlinelibrary.com]

for the description of MA. All Peaks are present, with only minor deviations in positions and intensities. Comparing $A_{PC}(\omega)$ of MA derived from more sophisticated charge schemes, namely electrostatic potential (ESP) and natural bond orbital (NBO) charges with $A_{QM}(\omega)$ reveals that employing the 6-31G* basis set Mulliken and ESP charges result in similar spectra, whereas the spectrum based on NBO charges has the highest deviation (Supporting Information Figure S1). As Mulliken charges are the cheapest, fastest, and most easy accessible charges, we used only Mulliken charges for the rest of the calculations.

In Figure 1B, we show the dominant role of the carbonyl and the hydroxyl group. According to the literature,[16] the carbonyl stretching mode is observed at 1 655, 1 593, and 1 358 cm^{-1} and the C—O(H) stretching mode participated to the bands at 1 655, 1 346, 1 260, and 1 092 cm^{-1}. In accordance, LMD assigns large percentages of these peaks to CO stretching modes. As in the experiments, frequent proton transfer within the trajectory leads to an equal population of the tautomer with the proton bound to OA and OB, respectively. As a result, the contributions of the OA—C3 and the OB—C1 stretching vibrations to the total spectrum are the same, because both bonds frequently interchange from single bond to double bond.

The two tautomers of MA are indistinguishable. Therefore, we introduce a single deuteration at the hydroxyl carbon of MA (Figure 2) to obtain two distinguishable states connected by the proton transfer reaction. To validate our Mulliken partial charge model, we demonstrate the similarity of the calculated IR spectrum $A_{PC}(\omega)$ with $A_{QM}(\omega)$ (Supporting Information Figure S2). There is no experimental spectrum for MA with a single deuteration at the hydroxyl carbon reported in the literature for further validation.

3.9 | Identifying transient states by LMA

By introducing the deuteration of the hydroxyl carbon, the two tautomeric states of MA become distinguishable (Figure 2A). State A (Z-3-deutero-3-hydroxy-prop-2-en-al) is defined by the transient proton being bound to the deuterons proximal oxygen atom (OA). State B (Z-1-deutero-3-hydroxy-prop-2-en-al) is defined by the transient proton being bound to the deuterons distal oxygen atom (OB). Tracking the distance of the hydrogen atom H to each of these oxygen atoms within the QM simulation trajectory allows for state assignment of different geometries of the trajectory as shown in Figure 2A. Through state-dependent LMA, two separate IR-spectra (Figure 2B) are extracted that correspond to the two different states. The spectra shown in Figure 2B reflect the differences between the two states and enables to assign marker bands that are only present in one of the states. The key IR band of our focus is present in state A at 2290 cm^{-1} and in state B at 2150 cm^{-1}. Next, this identified marker band needs to be assigned to structural vibrational modes. The spectral band assignment is performed by both, BPF (Supporting Information SM1 [https://youtu.be/ombxxCvtUAw]) and LMD (inset of Figure 2B). The CD-D vibrational stretching mode ν(CD-D) shifts by −140 cm^{-1} from states A to B. This band shift is in accordance with the one observed by NMA of −130 cm^{-1} for ν(CD-D). The band

assignment of ν(CD-D) is already extensively discussed in the literature.[16,18,19]

State-dependent LMA also identifies the proton transfer in the none-deuterated MA and now enables a clear-cut assignment of the contribution of the aldehyde (C═O) and the alcohol group (C—H), as shown in the Supporting Information Figure S3.

To represent the through LMA obtained correlation between structural changes in the trajectory and their spectral impact within the different states, we overlay the time-resolved spectrum with the average bond length between oxygen and proton of state B (Figure 3). Each time, windows reveal a very good correlation between the average bond length and the position of the marker bands. All in all, the correlation between state and band is clearly demonstrated by LMA. This allows also for the reverse approach, the assignment of states within a trajectory based on the presence of a marker band in the time-resolved LMA. The correlation of structural and spectral features can be an essential contribution for understanding experimental spectra and molecular mechanisms.
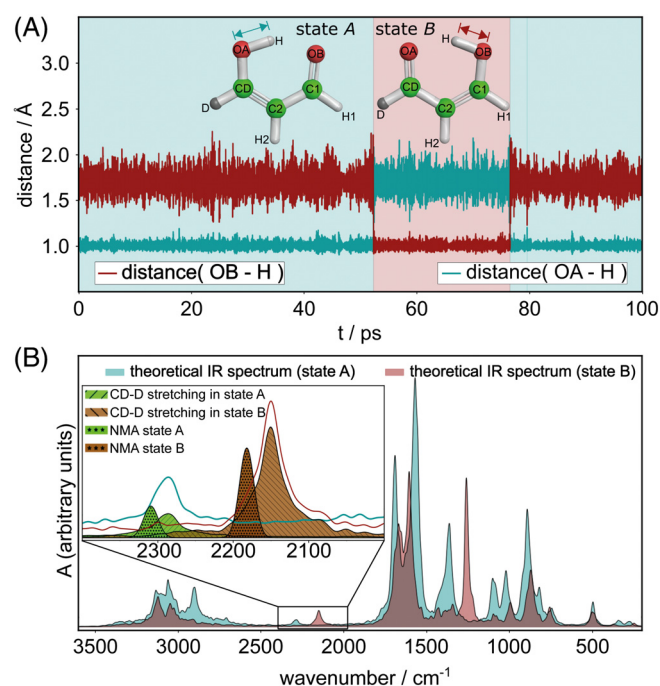

FIGURE 2 State assignment of proton transfer of C3-deuterated MA out of a QM trajectory. A, We identified two different states within a 100 ps QM simulation of C3-deuterated MA based on the distance over time plot of the proton-oxygen distance. In state A (cyan) the distance between the hydrogen atom H and the oxygen atom OA is below 1.2 Å and in state B (red) the distance between the hydrogen atom H and the oxygen atom OB is below 1.2 Å. B, Using state-dependent LMA, we obtained two state dependent IR spectra. The bands (2 290 cm^{-1} state A and 2 150 cm^{-1} state B) that only appear in one of the states are used as marker bands. The decomposition of these marker bands through LMD reveals that the bands are mainly evoked by the ν(CD-D) stretching vibrational mode as shown in the inset. The ν(CD-D) marker band differs by −140 cm^{-1} between states A and B, which is in accordance with the shift of −130 cm^{-1} calculated by NMA [Color figure can be viewed at wileyonlinelibrary.com]
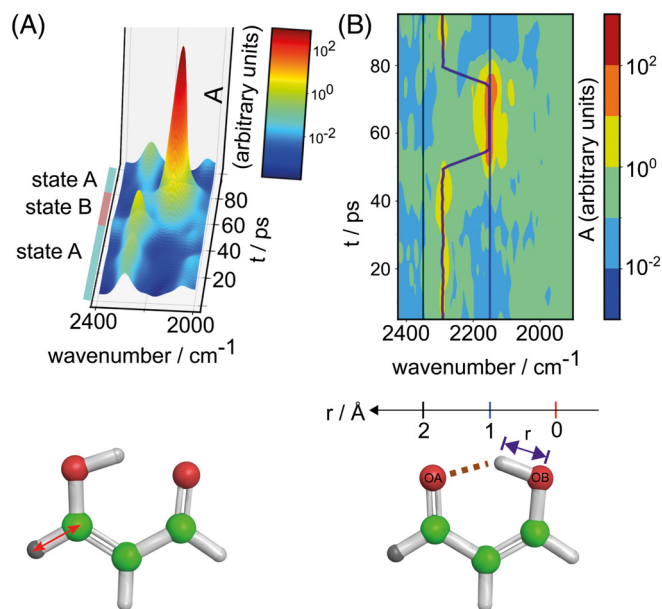
FIGURE 3 Correlation of marker band and the distance between the proton and the respective oxygen atom. A, 3D representation of the IR-spectrum over the time course zoomed to the in Figure 2B identified marker bands with its assignment shown in the structure below. B, 2D heat map representation of the 3D spectrum in A combined with the mean distance of the proton from OB in each time window (purple path). A very strong correlation of this distance with the shift of the marker band in time is observed

4 | CONCLUSIONS

We have developed and successfully applied a python-based software tool for LMA to correlate molecular details with spectral features and vice versa. LMD calculates IR spectra for atom groups or a single atom, which implies a decomposition and visualization of the contributions of the structural motions to the total IR spectrum. Band-pass filtering visualizes vibrational modes belonging to observed IR-bands. The visualization of spectral information through intuitive dynamic structural models makes the otherwise difficult to interpret IR spectroscopic results readily available to structural chemistry and biology.

The new features of time-resolved and state-dependent LMA enables to analyze also spectra of mixtures of different states or experimental time-resolved FTIR spectra of chemical reactions. Thus, LMA is suited to answer the questions about protein function that arise when measuring IR spectra of molecular systems.

The application to the simple but commonly used case of proton transfer in MA serves as prove of principle for time-resolved and state-dependent LMA. More complex systems than MA likely need longer QM trajectories to allow for sampling of the less frequently populated conformations. Through the continuous raise of computer power, larger molecular systems become available to be studied by molecular simulations.[42] The associated progress in hybrid method development combining QM with MM simulation allows studying active sites in small enzymes and large macromolecular complexes.[43] Thus, LMA is well suited as an IR spectroscopy tool applicable for almost all kinds of molecular systems. We anticipate LMA to be

beneficial to evaluate spectra and to initiate further experiments to test hypotheses about underlying protein function.

Software Availability

The LMA code is available under an MIT license and a user can flexibly adapt the code according to the individual needs by importing the LMA python package. The most recent version is available for download at https://github.com/MatthiasMa/Local-Mode-Analysis. Up-to-date information are provided at http://www.bph.rub.de/link_software_en.htm.

ORCID

Jürgen Schlitter 🄳 https://orcid.org/0000-0001-7310-874X
Carsten Kötting 🄳 https://orcid.org/0000-0002-3599-9657
Till Rudack 🄳 https://orcid.org/0000-0003-2693-9561
Klaus Gewert 🄳 https://orcid.org/0000-0001-8759-5964

REFERENCES

1. Kötting C, Gerwert K. Proteins in action monitored by time-resolved FTIR spectroscopy. *Chemphyschem*. 2005;6:881-888.
2. Wang JH, Xiao DG, Deng H, Callender R, Webb MR. Vibrational study of phosphate modes in GDP and GTP and their interaction with magnesium in aqueous solution. *Biospectroscopy*. 1998;4:219-227.
3. Rudack T, Jenrich S, Brucker S, Vetter IR, Gerwert K, Kötting C. Catalysis of GTP hydrolysis by small GTPases at atomic detail by integration of X-ray crystallography, experimental, and theoretical IR spectroscopy. *J Biol Chem*. 2015;290:24079-24090.
4. Mann D, Teuber C, Tennigkeit SA, Schröter G, Gerwert K, Kötting C. Mechanism of the intrinsic arginine finger in heterotrimeric G proteins. *Proc Natl Acad Sci*. 2016;1:201612394.
5. Rudack T, Xia F, Schlitter J, Kötting C, Gerwert K. Ras and GTPase-activating protein (GAP) drive GTP into a precatalytic state as revealed by combining FTIR and biomolecular simulations. *Proc Natl Acad Sci U S A*. 2012;109:15295-15300.
6. Schwoerer M, Wichmann C, Tavan P. A polarizable QM/MM approach to the molecular dynamics of amide groups solvated in water. *J Chem Phys*. 2016;144:114504. https://doi.org/10.1063/1.4943972
7. Thomas M, Brehm M, Fligg R, Vöhringer P, Kirchner B. Computing vibrational spectra from ab initio molecular dynamics. *Phys Chem Chem Phys*. 2013;15:6608-6622.
8. Mathias G, Baer MD. Generalized normal coordinates for the vibrational analysis of molecular dynamics simulations. *J Chem Theory Comput*. 2011;7:2028-2039.
9. Sun J, Bousquet D, Forbert H, Marx D. Glycine in aqueous solution: solvation shells, interfacial water, and vibrational spectroscopy from ab initio molecular dynamics. *J Chem Phys*. 2010;133:114508.
10. Kubelka J, Keiderling TA. Ab initio calculation of amide carbonyl stretch vibrational frequencies in solution with modified basis sets. 1. N-methyl Acetamide. *J Phys Chem A*. 2001;105:10922-10928.
11. Rudack T, Xia F, Schlitter J, Kötting C, Gerwert K. The role of magnesium for geometry and charge in GTP hydrolysis, revealed by quantum mechanics/molecular mechanics simulations. *Biophys J*. 2012;103:293-302.
12. Khrenova MG, Grigorenko BL, Nemukhin AV. Theoretical vibrational spectroscopy of intermediates and the reaction mechanism of the guanosine triphosphate hydrolysis by the protein complex Ras-GAP. *Spectrochim Acta - Part Mol Biomol Spectrosc*. 2016;166:68-72.

13. Gerwert K, Freier E, Wolf S. The role of protein-bound water molecules in microbial rhodopsins. *Biochim Biophys Acta - Bioenerg*. 2014; 1837:606-613.

14. Gerwert K, Mann D, Kötting C. Common mechanisms of catalysis in small and heterotrimeric GTPases and their respective GAPs. *Biol Chem*. 2017;398:523-533.

15. Massarczyk M, Rudack T, Schlitter J, Kuhne J, Kötting C, Gerwert K. Local mode analysis: decoding IR spectra by visualizing molecular details. *J Phys Chem B*. 2017;121:3483-3492.

16. Tayyari SF, Milani-Nejad F. On the reassignment of vibrational frequencies of malonaldehyde. *Spectrochim Acta A*. 1998;54:255-263.

17. Barone V. Vibrational zero-point energies and thermodynamic functions beyond the harmonic approximation. *J Chem Phys*. 2004;120: 3059-3065.

18. Terranova ZL, Corcelli SA. Monitoring intramolecular proton transfer with two-dimensional infrared spectroscopy: a computational prediction. *J Phys Chem Lett*. 2012;3:1842-1846.

19. Smith Z, Wilson EB, Duerst RW. The infrared spectrum of gaseous malonaldehyde (3-hydroxy-2-propenal). *Spectrochim Acta Part A*. 1983;39:1117-1129.

20. Pitsevich GA, Malevich AE, Kozlovskaya EN, et al. Theoretical study of the C-H/O-H stretching vibrations in malonaldehyde. *Spectrochim Acta Part A*. 2015;145:384-393.

21. Duan C, Luckhaus D. High resolution IR-diode laser jet spectroscopy of malonaldehyde. *Chem Phys Lett*. 2004;391:129-133.

22. Frisch MJ, Scheiner AC, Schaefer HF, Binkley JS. The malonaldehyde equilibrium geometry: a major structural shift due to the effects of electron correlation. *J Chem Phys*. 1985;82:4194-4198.

23. Carrington T, Miller WH. Reaction surface description of intramolecular hydrogen atom transfer in malonaldehyde. *J Chem Phys*. 1986;84: 4364-4370.

24. Tew DP, Handy NC, Carter S. A reaction surface Hamiltonian study of malonaldehyde. *J Chem Phys*. 2006;125:084313.

25. Kumar M, Finney BA, Francisco JS. Intramolecular hydrogen bonding in malonaldehyde and its radical analogues. *J Chem Phys*. 2017;147: 124309.

26. Sobolewski AL, Domcke W. On the mechanism of rapid non-radiative decay in intramolecularly hydrogen-bonded π systems. *Chem. Phys. Lett.* 1999;300:533-539.

27. Fillaux F, Nicolaï B. Proton transfer in malonaldehyde: from reaction path to Schrödinger's cat. *Chem Phys Lett*. 2005;415:357-361.

28. Wassermann TN, Luckhaus D, Coussan S, Suhm MA. Proton tunneling estimates for malonaldehyde vibrations from supersonic jet and matrix quenching experiments. *Phys Chem Chem Phys PCCP*. 2006;8: 2344-2348.

29. Huang J, Buchowiecki M, Nagy T, Vaníček J, Meuwly M. Kinetic isotope effect in malonaldehyde determined from path integral Monte Carlo simulations. *Phys Chem Chem Phys*. 2014;16:204-211.

30. Woodford JN. Density functional theory and atoms-in-molecules investigation of intramolecular hydrogen bonding in derivatives of malonaldehyde and implications for resonance-assisted hydrogen bonding. *J Phys Chem A*. 2007;111:8519-8530.

31. Ufimtsev IS, Martinez TJ. Quantum chemistry on graphical processing units. 3. Analytical energy gradients and first principles molecular dynamics. *J Chem Theor Comput*. 2009;5:2619-2628.

32. Schneider T, Stoll E. Molecular-dynamics study of a three-dimensional one-component model for distortive phase transitions. *Phys Rev B*. 1978;17:1302-1322.

33. Mulliken RS. Electronic population analysis on LCAO-MO molecular wave functions. I *J Chem Phys*. 1955;23:1833-1840.

34. Cooley BJW, Tukey JW. An algorithm for the machine calculation of complex Fourier series. *Math Comput*. 1965;19:297-301.

35. Russell D, Johnson III NIST Computational Chemistry Comparison and Benchmark Database NIST Standard Reference Database Number 101 Release 17b, September 2015. https://cccbdb.nist.gov/vibscale2.asp?method=8&basis=1. Accessed April 10, 2018.

36. Hariharan PC, Pople JA. The influence of polarization functions on molecular orbital hydrogenation energies. *Theor Chim Acta*. 1973;28: 213-222.

37. Van Der Walt S, Colbert SC, Varoquaux G. The NumPy array: a structure for efficient numerical computation. *Comput. Sci. Eng.* 2011;13: 22-30.

38. McGibbon RT, Beauchamp KA, Harrigan MP, et al. MDTraj: a modern open library for the analysis of molecular dynamics trajectories. *Biophys J*. 2015;109:1528-1532.

39. Hunter JD. Matplotlib: a 2D graphics environment. *Comput Sci Eng*. 2007;9:99-104.

40. Brewer, CA. (2017) COLORBREWER http://www.ColorBrewer.org. Accessed April 10, 2018.

41. Schrödinger, LLC (2015) The PyMOL Molecular Graphics System, Version 1.8.

42. Perilla JR, Goh BC, Cassidy CK, et al. Molecular dynamics simulations of large macromolecular complexes. *Curr Opin Struct Biol*. 2015;31:64-74.

43. Melo MCR, Bernardi RC, Rudack T, et al. NAMD goes quantum: an integrative suite for hybrid simulation. *Nat Methods*. 2018;15:351-354.

SUPPORTING INFORMATION

Additional supporting information may be found online in the Supporting Information section at the end of the article.